TABLE I. Clinical Features of Patients With a 9q34.1-qter Duplication

Phenotypic features	Gawlik-Kuklinska et al. [2007]	Youngs et al. [2010]	Patient 1	Patient 2
General				
Hypotonia	+	+	+	+
Failure to thrive	+	−	−	−
Intellectual disability	Mild	Mild	Mild	Mild
Cardiac anomalies	−	+	+	−
Overweight/obesity	+	+	−	−
Scoliosis	+	−	−	−
Facial characteristics				
Dolichcephaly	+	+	−	−
Facial asymmetry	+	+	−	−
Narrow horizontal palpebral fissures	+	+	−	−
Deep-set eyes	+	+	−	−
Long nose	+	+	−	−
Prominent chin	+	+	−	−
Microstomia	+	+	+	+
Microretrognathia	+	+	+	+
Short philtrum	+	−	+	+
Round face	−	−	+	+
Hypertelorism	−	−	+	+
Depressed nasal bridge	−	−	+	+
Almond-shape palpebral fissures	−	−	+	+
Telecanthus	−	−	+	+
Short nose	−	−	+	+
Extremities				
Long and thin fingers	+	+	+	+
Increased space between first and second toes	+	+	+	+

+, present; −, absent.

MATERIALS AND METHODS

Cytogenetic Analysis

Cultured lymphoblastoid cells isolated from each patient were treated with colchicine (Sigma–Aldrich, St. Louis, MO) for 1 hr at a concentration of 20 ng/ml in culture medium, and then incubated in a hypotonic solution of 75 mM KCl at 37°C for 30 min. After incubation, cells were fixed with Carnoy's fixative (3:1 mixture of methanol and acetic acid), spread on glass slides in a humid atmosphere and air-dried. Chromosomal analysis was carried out on GTG banded chromosomes at a resolution of 400–550 bands. Fluorescence in situ hybridization (FISH) was performed on metaphase chromosome spreads from each patient. Commercial probes covering subtelomeric regions were used according to the manufacturer's protocols (ToTelVysion, Abbott Laboratories. Abbott Park, IL) [Flint et al., 1995]. In order to confirm the chromosomal rearrangement in detail, additional FISH analysis was carried out from the patients and their parents using a series of bacterial artificial chromosome (BAC) clones (Clontech Laboratories, Inc., Mountain View, CA) that map to chromosome regions 9q34 and 13q31.

Array CGH Analysis

Genomic DNA was isolated from peripheral blood lymphocytes of the two patients, their parents, and three normal controls by phenol/chloroform extraction. Array CGH analysis was performed using the Agilent Human Genome CGH 244K microarray platform (Agilent Technologies, Santa Clara, CA) according to standard protocols provided by the manufacturer. This array spans the entire human genome at a median resolution of approximately 8.9 kb. Genomic copy numbers were analyzed with Genomic Workbench (Standard Edition 5.0.14; Agilent Technologies).

Southern Blot Analysis

Genomic DNA samples (10 µg) from the patients, their parents, and the normal controls were digested with HindIII, separated on a 0.9% agarose gel, and transferred by the alkaline method to a nylon membrane (Hybond-N+; GE Healthcare, Tokyo, Japan). The membrane was sequentially hybridized with [α-^{32}P]dCTP-labeled ABCA6 (exons 17–19) and SP2 (exons 4–7) cDNA. A 301 bp ABCA6 or a 798 bp SP2 cDNA probe was prepared by amplifying the cDNA library of human lymphoblastoid cells with AmpliTaq-

Gold (Applied Biosystems, Foster City, CA) using specific primer pairs for *ABCA6* (sense: 5′-ATCTTTTCAGTGATCTGGATAAG-3′; antisense: 5′-AGGGTCAATAACACTTTAGTTT-3′), and for *SP2* (sense: 5′-GTCTACATCCGCACGCCTTC-3′; antisense: 5′-CCGCCGCAGTTGGCCTTA-3′), respectively. The PCR products were subcloned into pGEM-T easy vector (Promega, Madison, WI), and the nucleotide sequence of the probes was confirmed. Hybridization was performed in hybridization solution containing 5× standard saline citrate (SSC), 5× Denhardt's solution, and 0.5% SDS at 66°C overnight. The membrane was washed three times with 2× SSC containing 0.1% SDS at 37°C for 20 min and once with 0.1× SSC containing 0.1% SDS at 55°C for 10 min, and then radioactivity was quantified with a BAS 1800 image analyzer (FUJIFILM, Tokyo, Japan). The radioactivity of *ABCA6* versus *SP2* was determined for both patients and their parents (RP1, RP2, RF, RM) relative to the mean of the three normal controls (RC).

RESULTS

Additional 9q Subtelomeric Signal

The G-banding pattern of the both patients showed a 46,XX normal female karyotype. FISH with probes for subtelomeric regions revealed an additional 9q subtelomeric signal on the short arm of a D-group chromosome (chromosome 13, 14, or 15) in both patients (data not shown).

9q34 Duplication

To assess the chromosomal rearrangements in more detail, FISH analysis was performed in both patients and their parents with three BAC clones (RP11-40A7 and RP11-81N19) from chromosome 9q34 and RP11-524C15 from chromosome 13q31. The result indicated that the mother had a translocation; a 9q34.1-qter segment from one chromosome 9 was translocated to the terminus of chromosome 13p (Fig. 2, lower panel, indicated by a yellow arrow). Both patients had two normal chromosomes 9 and the derivative chromosome 13, which had an additional 9q34.1-qter segment at the p-terminal (Fig. 2, lower panels, indicated by yellow arrows). The father did not show any abnormalities (data not shown). These results indicate that the additional 9q34.1-qter segment at the p-terminal of chromosome 13 was of maternal origin (Fig. 2). The breakpoint of the translocation fell between two BAC clones at RP11-81N19 (129.2 Mb from the 9p terminus) and RP11-40A7 (133.4 Mb). Detailed mapping of the 13p breakpoint is not necessary because 13p does not code any genes. Thus, the duplicated segment was estimated to be 6.8–11.0 Mb derived from the 9q-terminus at position 140.2 Mb [46,XX.ish der(13)t(9;13)-(q34.1;pter)mat] (Fig. 2).

8.5 Mb Duplication of 9q34.1-qter

We performed array CGH using genomic DNA from each patient to determine the precise size of the additional 9q34 segment and
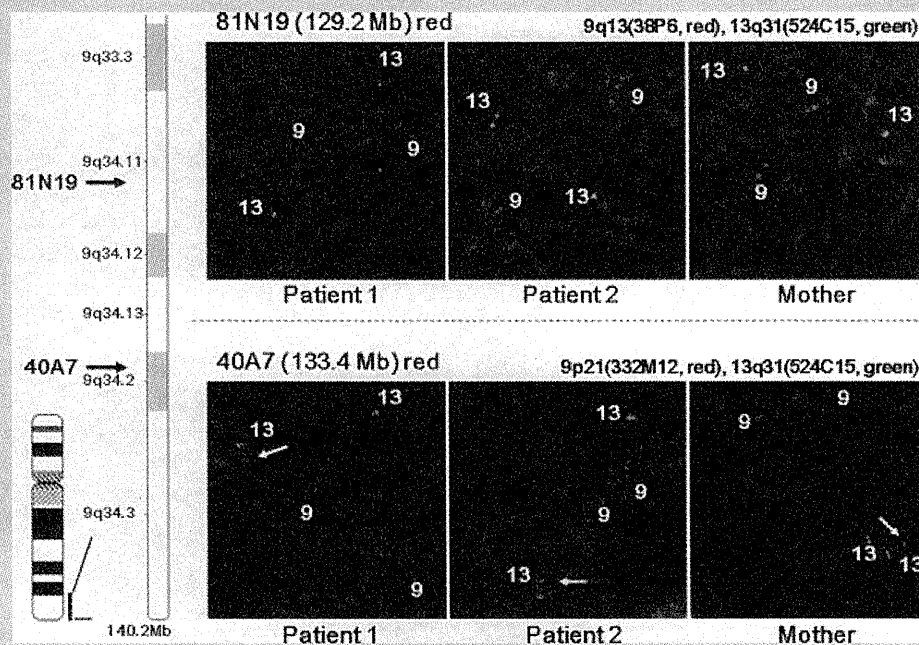

FIG. 2. Partial metaphases of FISH with BAC clone RP11-81N19 probe show two red signals on both 9q terminal regions of the mother and each patient (upper panel) and no signal on chromosome 13. Partial metaphases of FISH with BAC clone RP11-40A7 probe show a red signal on one 9q terminal region and the short arm of derivative chromosome 13 (yellow arrow) in the mother and three signals in both patients; two red signals on both 9q terminal regions and an additional signal on the short arm of derivative chromosome 13 (yellow arrow) (lower panel). RP11-38P6 (red), RP11-332M12 (red), and RP11-524C15 (green) are used as markers for 9q13, 9p21, and 13q31, respectively.

identify any other genomic abnormalities. Array CGH analysis of samples from Patients 1 and 2 demonstrated that the genomic copy number of 9q34.1-qter was 1.5-fold higher than the normal region (Fig. 3A,B). The size of the 9q34.1-qter duplication in both patients was approximately 8.5 Mb, from positions 131.7 to 140.2 Mb of chromosome 9 (Fig. 3). The breakpoint (position 131.7 Mb) of the 9q34 duplication in both patients was located in *FNBP1*, which encodes formin-binding protein 1. Analyses of Patients 1 and 2 revealed 12 and 15 copy number variations (CNVs), respectively (data not shown). CNVs are generally defined as the copy number differences of genomic DNA larger than 1 kb that vary in copy number between individuals. Patients 1 and 2 both had a 0.5-fold decrease in the genomic copy number of *ABCA6*, which encodes ATP-binding cassette, sub-family A, member 6; this is not recognized as a CNV (MIM 612504; Supplemental Fig. A and B).

ABCA6 Deletion in Both Patients and Their Mother

To confirm whether *ABCA6* was deleted in both patients and their parents, we performed Southern blot analysis using two cDNA probes against *ABCA6* (exons 17–19) and *SP2* (exons 4–7). *SP2* maps to 17q21, approximately 21 Mb proximal to *ABCA6*, and was not deleted in either patient based on the array CGH analysis. Southern blot analysis showed a decreased radioactive signal from *ABCA6* in family members (Supplemental Fig. C). When the mean ratio of *ABCA6* signal to *SP2* signal of the three normal controls was defined as 1.0, the ratio of *ABCA6* signal to *SP2* signal of the patients and their mother was approximately 0.5 and their father was 0.85

(Supplemental Fig. D). Thus, the both patients and their mother were heterozygous for an *ABCA6* deletion.

DISCUSSION

Duplications of 9q34 cause intellectual disability and multiple congenital anomalies. Reported cases presented with a variety of clinical features depending on the size of the duplication and the presence of other chromosomal abnormalities [Allderdice et al., 1983; Hodou et al., 1987; Spinner et al., 1993; Gawlik-Kuklinska et al., 2007; Youngs et al., 2010]. Our patients had a 9q34.1-qter duplication and partial 13p monosomy due to a translocation between 9q34.1 and 13pter in their healthy mother. Array CGH and Southern blot analyses confirmed that these patients had a 9q34.1-qter duplication and a heterozygous deletion of *ABCA6* (17q24). Because 13p does not code for any genes and the heterozygous deletion of *ABCA6* did not cause any phenotypic abnormalities in the mother, the present patients exhibited "pure" 9q34.1-qter duplications without any other chromosomal abnormalities involving coding genes.

9q34 duplication has been analyzed in detail using array CGH in only two other patients. Gawlik-Kuklinska et al. [2007] reported the case of the female with a 7.4 Mb (RP11-269P11 to RP11-295G24; 127.3–134.7 Mb) duplication of 9q34.1-q34.3 (Fig. 4) and compared the patient's clinical features to those of previously reported 9q34 duplication cases [Spinner et al., 1993], including a male patient later shown to have a 13.8 Mb (126.4–140.2 Mb) duplication of 9q33.3-qter [Youngs et al., 2010] (Fig. 4). The following
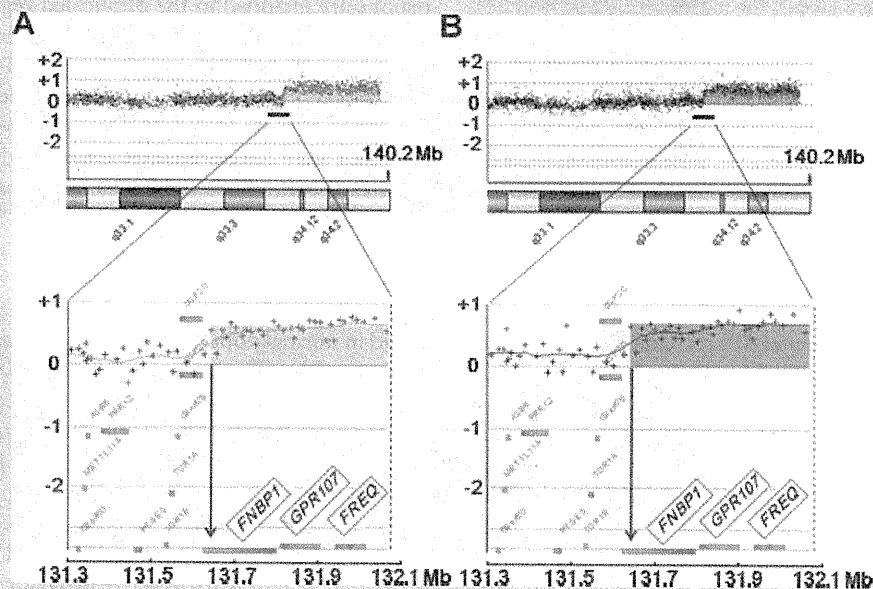

FIG. 3. A: Graphical representation of the results of the array CGH analysis (Agilent 244K oligonucleotide array) from Patient 1 shows the duplication of distal 9q34.1-qter (upper panel). The x- and y-axis denote genomic position and log₂ ratio, respectively. B: Graphical representation of the results of the array CGH analysis from Patient 2 also shows the duplication of distal 9q34.1-qter (upper panel). The breakpoint in 9q34 was located in the *FNBP1* gene (131.7 Mb) in both patients (lower panels of A and B), which indicated that the size of the duplication was approximately 8.5 Mb (131.7–140.2 Mb) according to NCBI human genome build 36.3.
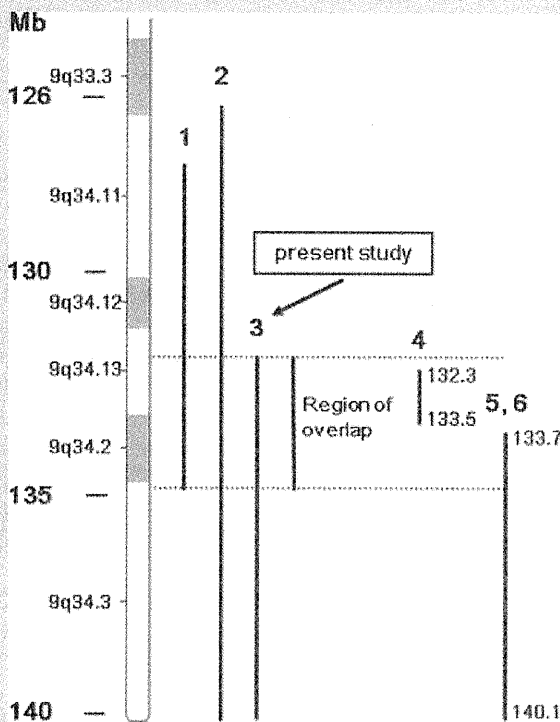
FIG. 4. A schematic illustration based on NCBI human genome build 36.3 of 9q34 duplications from two previously reported cases, the present patients, and three patients from DECIPHER. The duplications in the previously reported patients and our patients are denoted as 1 (127.3–134.7 Mb) [Gawlik-Kuklinska et al., 2007], 2 (126.4–140.2 Mb) [Youngs et al., 2010], and 3 (131.7–140.2 Mb) [present study]. The 3.0 Mb (131.7–134.7 Mb) overlapping region of all three 9q34 duplications is denoted as "Region of overlap." The duplications in the patients from DECIPHER are denoted as 4 (P253579; age 1?, 46,XX) (132.3–133.5 Mb), 5 (P254131; age 2, 46,XX) (133.7–140.1 Mb), and 6 (P255167; age 2, 46,XY) (133.7–140.1 Mb).

patients (Fig. 4, Table I). Unlike the other patients, our patients did not have dolichocephaly, facial asymmetry, narrow palpebral fissures, deep-set eyes, or long nose. The locus or loci associated with these phenotypes may be located in a region (127.3–131.7 Mb) that is proximal to the overlapping region (Fig. 4, Table I). Our patients exhibited other characteristic facial features, such as round faces, hypertelorism, almond-shaped palpebral fissures, telecanthus, and short nose; those were not observed in the previously reported cases (Table I). The distal-most segment of 9q34 (134.7–140.2 Mb) in our patients is the strongest candidate for the origin of these phenotypes (Fig. 4). However, these phenotypes were not observed in Patient 2 [Youngs et al., 2010], who had the same 9qter duplication. Therefore, the duplication of the proximal segment (127.3–131.7 Mb) of the overlapping region may have more impact on facial appearance than the duplication of the distal segment of the overlapping region. Clinical analyses of more patients with 9qter duplication (134.7–140.2 Mb) are necessary to determine the phenotypes caused by duplication of this region. It should be noted that DECIPHER (Database of Chromosomal Imbalance and Phenotype in Human using Ensembl Resources) includes two patients (P254131 and P255167) with the same 9q34.2-qter duplication (133.7–140.1 Mb) and heterozygous deletion of 17pter (0.01–0.41 Mb) (Fig. 4, numbers 5, 6). These patients exhibited hypotonia (non-myopathic), intellectual disability, developmental delay, patchy café au lait pigmentation spots on the skin, and speech delay. The heterozygous 17pter 0.4 Mb deletion has not been reported to cause any diseases, including intellectual disability. Another patient (P253579) presenting with facial abnormality, intellectual disability, and developmental delay had a 9q34.1-q34.2 duplication (132.3–133.5 Mb) in the 3.0 Mb overlapping region (Fig. 4, number 4). Notably, these two duplicated regions are included in the duplicated region in our patients, but they do not overlap with each other. These findings suggest the following correlations between duplicated chromosomal segments of 9q34 and phenotypes: (1) two duplicated segments (133.7–140.1 and 132.3–133.5 Mb) in 9q34 are associated with intellectual disability and developmental delay; and (2) the locus or loci associated with characteristic facial appearance may be within a duplicated region of 1.2 Mb (132.3–133.5 Mb), even though the detailed clinical features of P253579 are not available. Of the 18 genes that map to this 1.2 Mb region, individual duplications of 12 genes are reported in the Database of Genomic Variants (DGV; found in normal population). Thus, increased copy number of one or more of the other six genes (FUBP3, EXOSC2, ABL1, NUP214, FAM78A, and PPAPDC3) in this region could be the cause of the intellectual disability, developmental delay, and characteristic facial appearance observed in our patients and P253579.

Chromosomal rearrangements, arising from unequal recombination between repeated sequences, are found in a subset of patients with autism spectrum disorder [Marshall et al., 2008]. Abnormal behaviors, including hyperactive behavior [Allderdice et al., 1983], food-seeking behavior [Gawlik-Kuklinska et al., 2007], hyperactivity, attention deficit disorders, and atypical autism [Youngs et al., 2010], were also reported in some patients with 9q34 duplication. Unlike these patients, our patients exhibited friendly and affectionate social behaviors and did not exhibit autistic features or attention deficit disorder. It is important to repeatedly monitor the behaviors

features were common to both patients in these reports: hypotonia, intellectual disability, developmental delay, characteristic head and facial features associated with dolichocephaly, facial asymmetry, narrow palpebral fissures, deep-set eyes, long nose, prominent chin, microstomia, microretrognathia, and characteristic features of the extremities, including long thin fingers and toes and camptodactyly (Table I). Gawlik-Kuklinska et al. [2007] concluded a 7.4 Mb (127.3–134.7 Mb) duplicated region in their patient was critical for the phenotypes they observed (Fig. 4). Like these two previously reported cases, our patients also exhibited hypotonia, mild intellectual disability, developmental delay, microstomia, microretrognathia, and long thin fingers and toes. Thus, the 3.0 Mb region (131.7–134.7 Mb) of 9q34.13-q34.3 that overlapped in the cases reported by previous studies [Gawlik-Kuklinska et al., 2007; Youngs et al., 2010], and in our patients is most likely associated with the manifestation of the phenotypes observed in all four

of our patients to determine whether the 9q34.1-qter duplication is associated with abnormal behaviors. In summary, our findings indicate that the duplication of 9q34 is a heterogeneous clinical condition and duplications of different segments of 9q34 are associated with a variety of symptoms. Genomic and clinical analyses of more patients carrying 9q34 duplications are necessary to better characterize the correlation between clinical phenotypes and specific 9q34 loci.

ACKNOWLEDGMENTS

REFERENCES

Allderdice PW, Eales B, Onyett H, Sprague W, Henderson K, Lefeuvre PA, Pal G. 1983. Duplication 9q34 syndrome. Am J Hum Genet 35:1005–1019.

Flint J, Wilkie AO, Buckle VJ, Winter RM, Holland AJ, McDermid HE. 1995. The detection of subtelomeric chromosomal rearrangements in idiopathic mental retardation. Nat Genet 9:132–140.

Gawlik-Kuklinska K, Iliszko M, Wozniak A, Debiec-Rychter M, Kardas I, Wierzba J, Limon J. 2007. A girl with duplication 9q34 syndrome. Am J Med Genet Part A 143A:2019–2023.

Hodou S, Yorifugi T, Tsuruta S, Hashida K, Ohta S, Ieshima A. 1987. Distal 9q trisomy syndrome: Report of the first oriental case and literature review. Acta Neonatal Jpn 23:347–352.

Marshall CR, Noor A, Vincent JB, Lionel AC, Feuk L, Skaug J, Shago M, Moessner R, Pinto D, Ren Y, Thiruvahindrapduram B, Fiebig A, Schreiber S, Friedman J, Ketelaars CE, Vos YJ, Ficicioglu C, Kirkpatrick S, Nicolson R, Sloman L, Summers A, Gibbons CA, Teebi A, Chitayat D, Weksberg R, Thompson A, Vardy C, Crosbie V, Luscombe S, Baatjes R, Zwaigenbaum L, Roberts W, Fernandez B, Szatmari P, Scherer SW. 2008. Structural variation of chromosomes in autism spectrum disorder. Am J Hum Genet 82:477–488.

Spinner NB, Lucas JN, Poggensee M, Jacquette M, Schneider A. 1993. Duplication 9q34→qter identified by chromosome painting. Am J Med Genet 45:609–613.

Youngs EL, McCord T, Hellings JA, Spinner NB, Schneider A, Butler MG. 2010. An 18-year follow-up report on an infant with a duplication of 9q34. Am J Med Genet Part A 152A:230–233.

FULL-LENGTH ORIGINAL RESEARCH

CDKL5 alterations lead to early epileptic encephalopathy in both genders

*†‡Jao-Shwann Liang, *Keiko Shimojima, §Rumiko Takayama, ¶Jun Natsume, *†Minobu Shichiji, †Kyoko Hirasawa, †Kaoru Imai, #Tohru Okanishi, **Seiji Mizuno, ††Akihisa Okumura, *Midori Sugawara, §Tomoshiro Ito, §Hiroko Ikeda, §Yukitoshi Takahashi, †Hirokazu Oguni, §Katsumi Imai, †Makiko Osawa, and *Toshiyuki Yamamoto

*Tokyo Women's Medical University Institute for Integrated Medical Sciences, Tokyo, Japan; †Department of Pediatrics, Tokyo Women's Medical University, Tokyo, Japan; ‡Department of Pediatrics, Far Eastern Memorial Hospital, Taipei, Taiwan; §National Epilepsy Center, Shizuoka Institute of Epilepsy and Neurological Disorders, Shizuoka, Japan; ¶Department of Pediatrics, Nagoya University School of Medicine, Nagoya, Japan; #Department of Pediatrics, Seirei Hamamatsu Hospital, Hamamatsu, Japan; **Department of Medical Genetics, Aichi Prefectural Colony Central Hospital, Kasugai, Japan; and ††Department of Pediatrics, Juntendo University School of Medicine, Tokyo, Japan

SUMMARY

Purpose: Genetic mutations of the cyclin-dependent kinase-like 5 gene (*CDKL5*) have been reported in patients with epileptic encephalopathy, which is characterized by intractable seizures and severe-to-profound developmental delay. We investigated the clinical relevance of *CDKL5* alterations in both genders.

Methods: A total of 125 patients with epileptic encephalopathy were examined for genomic copy number aberrations, and 119 patients with no such aberrations were further examined for *CDKL5* mutations. Five patients with Rett syndrome, who did not show methyl CpG-binding protein 2 gene (*MECP2*) mutations, were also examined for *CDKL5* mutations.

Key Findings: One male and three female patients showed submicroscopic deletions including *CDKL5*, and two male and six female patients showed *CDKL5* nucleotide alterations. Development of early onset seizure was a characteristic clinical feature for the patients with *CDKL5* alterations in both genders despite polymorphous seizure types, including myoclonic seizures, tonic seizures, and spasms. Severe developmental delays and mild frontal lobe atrophies revealed by brain magnetic resonance imaging (MRI) were observed in almost all patients, and there was no gender difference in phenotypic features.

Significance: We observed that 5% of the male patients and 14% of the female patients with epileptic encephalopathy had *CDKL5* alterations. These findings indicate that alterations in *CDKL5* are associated with early epileptic encephalopathy in both female and male patients.

KEY WORDS: CDKL5, Epileptic encephalopathy, Genomic copy number aberration, Mutation, Gender.

Epileptic encephalopathies are a group of conditions in which neurologic deterioration results mainly from epileptic activity. The clinical and electroencephalography (EEG) characteristics depend on the age of onset and may change over time (Zupanc, 2009). An underlying genetic background has been suggested in patients with epileptic encephalopathy (Nabbout & Dulac, 2008). An X-linked gene coding for cyclin-dependent kinase-like 5 gene (*CDKL5*; MIM #300203) is one of the genes responsible for epileptic encephalopathy. Kalscheuer et al. (2003) identified de novo

balanced X autosome translocations in two female patients with infantile spasms, in whom *CDKL5* was disrupted. Since then, the phenotypic spectrum of *CDLK5* abnormalities has expanded to include features resembling Rett syndrome (RTT; MIM #312750) with early onset seizures (Evans et al., 2005; Mari et al., 2005). Now, phenotypic features of *CDLK5* abnormalities are widely recognized as early infantile epileptic encephalopathy-2 (EIEE-2; MIM #30062) and are characterized as severe epileptic encephalopathy associated with early onset and refractory seizures (Archer et al., 2006; Pintaudi et al., 2008).

Although the consequence of *CDKL5* alterations has also been attributed to X-linked dominant infantile spasm syndrome-2 (ISSX2), mutations have been identified not only in female patients but also in some male patients with severe mental retardation and early onset intractable seizures (Elia et al., 2008; Fichou et al., 2009; Sartori et al., 2009).

1

Therefore, we performed a comprehensive analysis for *CDKL5* in both female and male patients with epileptic encephalopathy.

METHODS

Patients

After obtaining approval of the study protocol by the ethics committee of the institution and informed consent from the families of the patients, peripheral blood samples of 125 patients (59 male and 66 female) with epileptic encephalopathy of unknown etiology were collected, together with their clinical information, including neuroimaging findings. Epileptic encephalopathies are defined as disorders in which there is a temporal relationship between deterioration in cognitive, sensory, and motor function and epileptic activity, which includes frequent seizures and/or extremely frequent interictal paroxysmal activity (Nabbout & Dulac, 2003). Five female patients with RTT who did not show methyl CpG-binding protein 2 gene (*MECP2*) mutations (which are often associated with RTT) were also included in the cohort study for *CDKL5* mutations.

Microarray-based comparative genomic hybridization (aCGH) analysis

The genomic copy numbers of the patients with epileptic encephalopathies were determined using the Human Genome CGH Microarray 105K (Agilent Technologies, Santa Clara, CA, U.S.A.) as described previously (Shimojima et al., 2010).

Validation of the genomic copy number aberrations

Fluorescent in situ hybridization (FISH) analysis was performed for the large chromosomal deletion by using bacterial artificial chromosome (BAC) clones as probes, RP11-106N3 and CTD-2335C24 including *CDKL5* as a target, and RP11-1051J20 as a marker (Fig. 1, Table S1). The deletion identified in Patient 1 was too small to be detected by a BAC clone; therefore, multiplex polymerase chain reaction (PCR) analysis was used for validation. Two DNA fragments, exon 1B (421 bp) and exon 2 (350 bp) of *CDKL5*, were amplified in the same PCR reaction tube, separated by agarose gel electrophoresis, and visualized by ethidium bromide staining.

Cohort study for *CDKL5*

Samples from 119 patients (58 male and 61 female) that showed no genomic copy number aberrations at the first screening by microarray-based comparative genomic hybridization (aCGH) in this study were included in the second cohort. Five samples obtained from female patients with RTT who did not show *MECP2* mutations were also included. The genomic sequences of all 23 exons of *CDKL5* were analyzed by the standard PCR direct-sequencing method using primers listed in Table S2. A recently
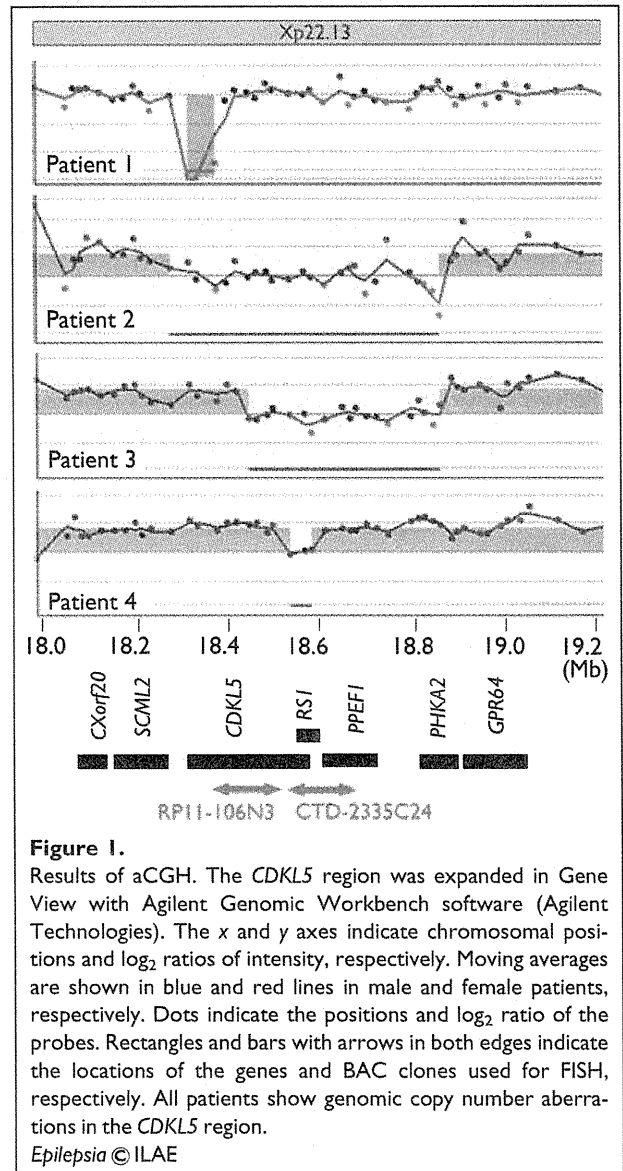
Figure 1.
Results of aCGH. The *CDKL5* region was expanded in Gene View with Agilent Genomic Workbench software (Agilent Technologies). The x and y axes indicate chromosomal positions and $\log_2$ ratios of intensity, respectively. Moving averages are shown in blue and red lines in male and female patients, respectively. Dots indicate the positions and $\log_2$ ratio of the probes. Rectangles and bars with arrows in both edges indicate the locations of the genes and BAC clones used for FISH, respectively. All patients show genomic copy number aberrations in the *CDKL5* region.
Epilepsia © ILAE

identified exon 16B, which if included in the mature mRNA produces as a new *CDKL5* isoform, was also analyzed in this study (Fichou et al., 2010). When nucleotide changes were identified in samples for which parental samples were available, trio analyses were performed to test whether the mutation was de novo or familial. DNA samples collected from 100 healthy Japanese volunteers (50 male and 50 female) comprised the control cohort.

RESULTS

Genomic copy number aberrations

In Patient 1, an aberration was identified at Xp22.13, indicating a nullisomy of this region (Fig. 1, Table S3). This region corresponds to exon 1 of *CDKL5*. Subsequent

multiplex PCR analysis using two sets of primers for exon 1B and exon 2 of *CDKL5* showed no band for exon 1B (Fig. 2A), thereby confirming the nullisomy of this region. Both parents of Patient 1 declined trio analysis.

aCGH analysis identified chromosomal aberrations in the *CDKL5* region in three female patients (Fig. 1, Table S3). Because male reference DNA was used in this study, genomic copy numbers of the normal female X chromosome regions showed $\log_2$ ratio of +1. Therefore, a $\log_2$ ratio of "0" indicates the same genomic copy numbers with the male reference sample, indicating a partial monosomy of this region in these patients. For Patients 2 and 3, identified aberrations were confirmed by FISH by detecting only one signal with RP11-106N3 and CTD-2335C24, respectively, indicating deletions in this region (Fig. 2B,C). For Patient 4, one of the targeted signals of CTD-2335C24 was weaker than the other, indicating a partial deletion of the targeted region (Fig. 2D). For Patients 2 and 3, the deletion region involved four genes: *CDKL5*; X-linked juvenile retinoschisis protein gene (*RS1*), which is responsible for X-linked

juvenile retinoschisis (MIM #312700); protein phosphatase with EF hand calcium-binding gene (*PPEF1*); and phosphorylase kinase alpha 2 gene (*PHKA2*), which is responsible for X-linked hepatic glycogen storage disease (MIM #300798). For Patient 3, the deleted region involved the
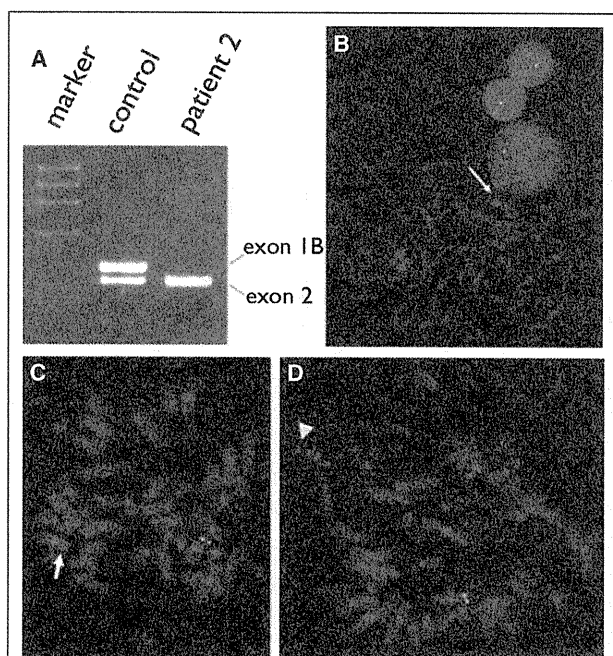

Figure 2.
Validations of genomic copy number aberrations. (**A**) Multiplex PCR amplification indicates deletion of exon 1B in Patient 1. The marker lane shows HaeIII digested φX174 DNA. (**B, C**) FISH analysis indicates loss of the green signal on one of the X chromosomes (arrows). For Patient 2 (**B**) and Patient 3 (**C**), RP11-106N3 and CTD-2335C24 are used for the targets, respectively. Patient 4 (**D**) shows a week green signal labeled on CTD-2335C24 (arrowhead), indicating a partial deletion within CTD-2335C24 region.
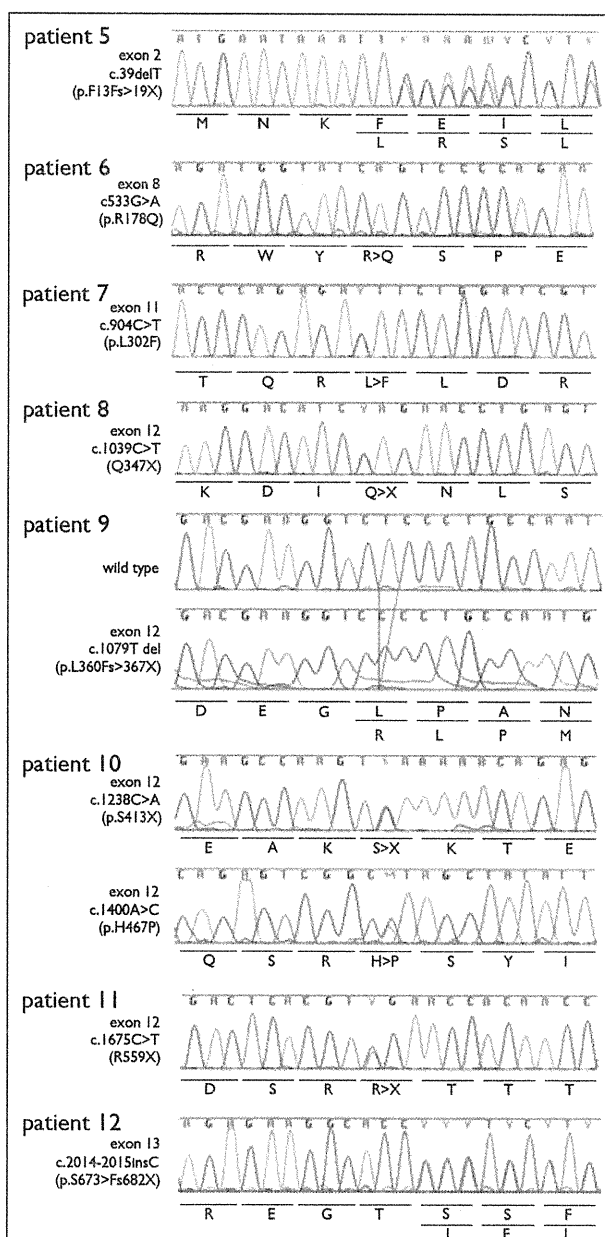*Epilepsia* © ILAE

Figure 3.
Electrophoresis of the direct sequencing. Alphabetic symbols indicate amino acids. For Patients 5, 9, and 12, lines above the sequences indicate reference amino acid sequences, and lines below the sequences indicate amino acid changes caused by the mutations.
Epilepsia © ILAE

Table 1. Summary of the clinical features and the identified *CDKL5* mutations in the patients reported in this study

No.	1	2	3	4	5	6	7	8	9	10	11	12
Gender	M	F	F	F	F	M	F	F	M	F	F	F
Initial concerns	EE	EE	EE	EE	EE	EE	EE	EE	EE	EE	EE	EE
Age at examination	6 m	2 y 7 m	4 y 2 m	2 y 7 m	8 m	1 y 9 m	4 y 7 m	2 y 6 m	2 y	2 y 1 m	1 y 4 m	1 y 4 m
Physical examination												
Birth weight (g)	3,458	3,016	2,400	2,716	2,612	3,800	2,560	3,352	3,228	2,955	3,250	2,976
OFC at birth (cm)	36.0	36.0	32.0	32.0	30.3	34.0	NT	NT	36.0	NT	33.0	33.5
Microcephaly	−	−	+	+	+	−	−	−	−	−	−	+
Deceleration of head growth	−	−	−	−	+	−	−	−	−	−	−	+
Neurologic features												
Hypotonia	−	−	+	+	+	+	+/−	+/−	+	+/−	+	+
Autistic features	NT	NT	+	NT	NT	−	+/−	+	NT	+	+	NT
Stereotype movement	NT	NT	+	+	+	−	−	+	NT	+	−	NT
Development												
Sitting	−	−	−	−	−	−	−	+	−	−	−	+
Walking	−	−	−	−	−	−	−	−	−	−	−	−
Best motor development	Bedridden	Bedridden	Turn over	Turn over	Bedridden	Bedridden	Bedridden	Sit	Bedridden	Turn over	Turn over	Sit
Speech	−	−	−	−	−	−	−	−	−	−	−	−
Seizure												
Age at onset of seizure	1 m	1 m	2 m	1.5 m	2 w	2 w	4 d	2 m	3 m	3 w	6 m	6 w
Persistent epilepsy	+	+	+	+	+	+	−	+	+	+	+	+
Seizure type	Infantile spasms	Infantile spasms	Spasms, focal Sz, myoclonia	Spasms, focal Sz	Spasms, focal Sz	Epileptic spasms	Infantile spasms	Tonic–clonic convulsion	Infantile spasms	Tonic–clonic convulsion	Tonic–clonic convulsion	Epileptic spasms
Radiologic examination												
Brain MRI	Cerebral atrophy	Cerebral atrophy	Cerebral atrophy	Mild cerebral atrophy	Cerebral atrophy	Bifrontal-diffuse atrophy	Very mild cerebral atrophy	Mild frontal lobe atrophy	Cerebral atrophy	Cerebral atrophy	Frontal lobe atrophy and delayed myelination	Mild cerebral atrophy
Hypoperfusion revealed by SPECT	NT	NT	Left frontal	NT	No abnormality	Right frontal	Right temporal	Left frontal	No abnormality	NT	Frontal and left parietal	NT

Continued

Table 1. Continued

No.	1	2	3	4	5	6	7	8	9	10	11	12	13
Mutation Location	Exon 1	Whole exons	Large deletion after exon 4	Large deletion after exon 16	Exon 2	Exon 8	Exon 11	Exon 12	Exon 12	Exon 12	Exon 12	Exon 12	Exon 13
Nucleotide change					c.39delT	c.533G>A	c.904C>T	c.1039C>T	c.1079delT	c.1238C>G	c.1400A>C	c.1675C>T	c.2014-2015insC
Amino acid change					p.F13Fs>19X	p.R178Q	p.L302F	p.Q347X	p.L360Fs>367X	p.S413X	p.H467P	p.R559X	p.S673>Fs682X
Domain						Catalytic							
Inheritance	NT	De novo	De novo	De novo	NT	De novo	NT	NT	NT	De novo	De novo	NT	De novo
Novel/recurrent	Novel	Novel	Novel	Novel	Novel	Novel	Novel	Recurrent	Novel	Novel	Novel	Recurrent	Novel
Population study	NT	NT	NT	NT	None	None	None	None	None	None	None	None	None
Previous reports								Aruso et al. (2010)				Sartori et al. (2009)	

M, male; F, female; EE, epileptic encephalopathy; y, years; m, months; w, weeks; d, days; OFC, occipitofrontal circumference; NT, not tested; Sz, seizures; SPECT, single-photon emission computed tomography.

latter half of CDKL5 after exon 4. Patient 4 also showed a partial CDKL5 deletion after exon 16, and RS1, which was encoded in the antisense direction. For Patients 2, 3, and 4, both parents were negative for these deletions, indicating de novo origin.

There were no other known pathogenic aberrations in these four patients. In the other two patients, genomic copy number aberrations in the region of the platelet-activating factor acetylhydrolase gene (PAFAH1B1), which is responsible for lissencephaly, were identified (Shimojima et al., 2010). The remaining 119 patients showed no genomic copy number aberrations and were included in the cohort study for CDKL5 mutations.

CDKL5 nucleotide alterations

In the 119 patients, eight pathogenic mutations were identified (including six novel and two recurrent mutations), which consisted of three nonsense mutations, three frameshift mutations, and two missense mutations (Fig. 3, Table 1). Aristaless-related homeobox gene (ARX; MIM #300382) was not found in any of the male patients. Five patients with RTT who did not show MECP2 mutations also did not show mutations in CDKL5. No control samples showed any of the nucleotide alterations identified in this study (Table 1).

Although Patient 10 showed a nonsense mutation (p.S413X), an additional missense mutation (p.H467P) was also identified in exon 12. Neither alteration was found in parents, indicating de novo occurrence of both mutations. Because a similar missense mutation (p.H467R) was reported to be a nonpathogenic mutation, p.H467P is also expected to be a nonpathogenic mutation (Evans et al., 2005).

Clinical description

Brain magnetic resonance imaging (MRI) of the patients with CDKL5 alterations is shown in Fig. 4. Many patients showed frontal dominant cerebral atrophy. All clinical data including the findings of neuroimaging are summarized in Table 1. The ability to sit autonomously was the maximum gross motor development achieved by these patients, and none of the patients acquired speech ability, indicating severe developmental delay. Only the oldest patient (Patient 7; 4 years and 7 months old), who had a missense mutation, showed seizure control after 3 years of age; all the other patients had persistent seizures.

DISCUSSION

Using aCGH analyses, Erez et al. (2009) identified partial CDKL5 deletions in female patients with early onset intractable epilepsy. Mei et al. (2010) identified four patients who had total or partial deletions in CDKL5. However, those studies included only female patients. In comparison, the aim of our study was to identify candidate
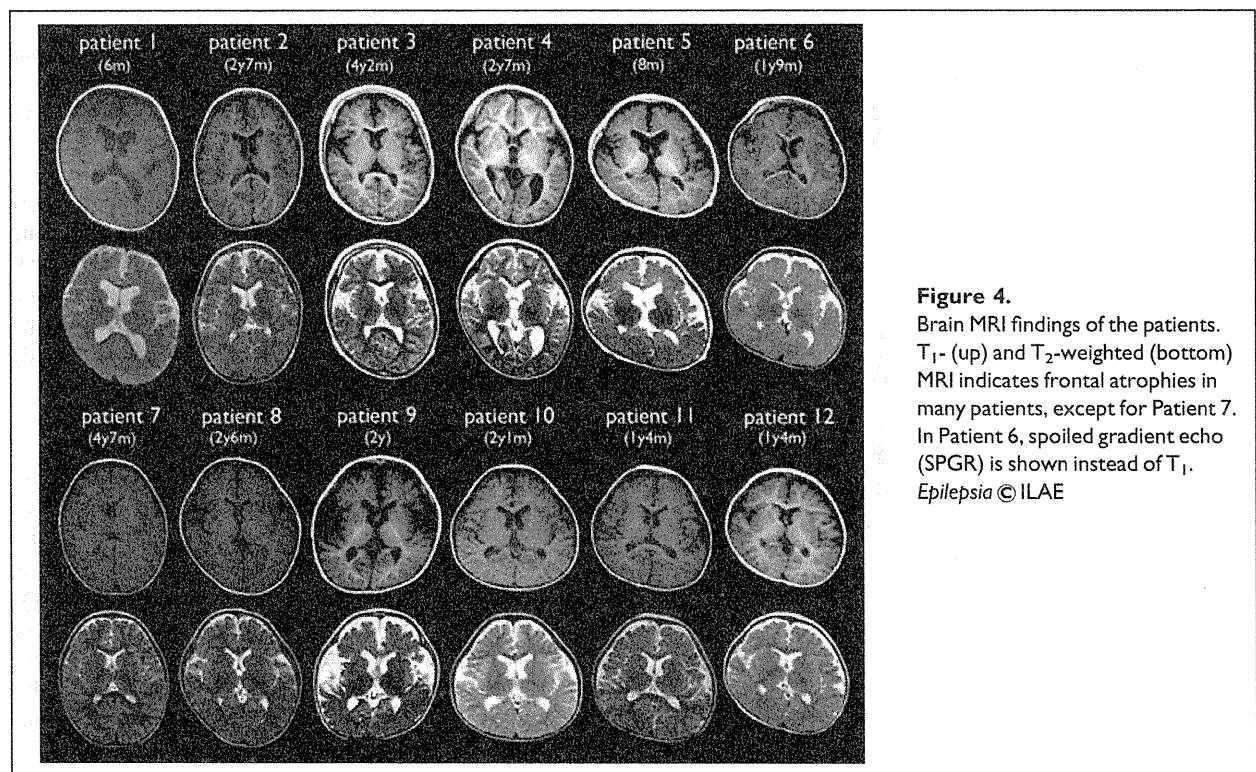
Figure 4.
Brain MRI findings of the patients.
T_1- (up) and T_2-weighted (bottom)
MRI indicates frontal atrophies in
many patients, except for Patient 7.
In Patient 6, spoiled gradient echo
(SPGR) is shown instead of T_1.
Epilepsia © ILAE

genetic causes of early epileptic encephalopathy, and thus we recruited patients of both genders. Genomic copy numbers of whole chromosomes were comprehensively analyzed and submicroscopic chromosomal abnormalities of the *CDKL5* region were identified in both genders. The male patient (Patient 1) showed a partial deletion of *CDKL5*. Patients 2 and 3 showed large deletions in which the four neighboring genes, *CDKL5*, *RS1*, *PPEF1*, and *PHKA2*, were included. *RS1* and *PHKA2* are responsible for X-linked diseases, and the function of *PPEF1* is unknown. The remaining Patient 4 showed partial deletions of *CDKL5* and *RS1*. Therefore, phenotypic features of Patients 2, 3, and 4 suggest a causal role for *CDKL5* deletions in early epileptic encephalopathy. Despite the gender difference and the deleted size differences, the clinical severities of the patients with *CDKL5* deletions were similar between genders and similar to those of patients previously reported to have partial or total deletion of *CDKL5* (Van Esch et al., 2007; Erez et al., 2009; Bahi-Buisson et al., 2010; Mei et al., 2010).

Previously, *CDKL5* mutations were shown to affect mainly female patients, and their frequency has been estimated as approximately 9–28% in female patients with early onset seizures (Bahi-Buisson et al., 2008b; Nemos et al., 2009). However, those studies mainly included female patients. Elia et al. (2008) identified *CDKL5* mutations in three male patients with early onset epileptic encephalopathy. Male patients with *CDKL5* mutations or

deletions have also been reported by others (Fichou et al., 2009; Sartori et al., 2009). In our study, initial identification of *CDKL5* deletions in both male and female patients with early epileptic encephalopathy prompted us to analyze *CDKL5* nucleotide sequences of both genders, and the results revealed nucleotide changes in two male patients and six female patients. We observed that the clinical severity of the disease did not differ between males and females. Therefore, male as well as female patients with early onset epileptic encephalopathy should be tested for *CDKL5* mutations.

Because *CDKL5* is located on Xp22.13, genetic traits of *CDKL5* alterations have been considered to be X-linked dominant, just as *MECP2* mutations are responsible for the majority of RTT cases, a neurologic disorder occurring almost exclusively in females. The rare male patients with *MECP2* mutations showed severe mental retardation but no RTT phenotype (Gomot et al., 2003). In comparison, there are no phenotypic differences between male and female patients with *CDKL5* mutations or deletions. Bahi-Buisson et al. (2008b) suggested that phenotypic heterogeneity does not correlate with the nature or the position of the mutations or with the pattern of X-chromosome inactivation. Indeed, no clear genotype–phenotype correlation between these factors has been established. Therefore, an important question is why clinical severity is the same between the genders. Based on previous reports, we know that the absence of CDKL5 protein is not lethal in males, and *CDKL5*

abnormalities result in severe neurodevelopmental delay and early onset epilepsy in both genders (Castren et al., 2011). In this study, the estimated frequencies of *CDKL5* abnormalities in patients with epileptic encephalopathy were 5% in male and 14% in female patients. Therefore, the observed difference in the frequency of *CDKL5* mutations between male and female patients may simply be a consequence of the fact that female patients have two X chromosomes.

Subjects in our study included five female patients with RTT who did not show *MECP2* mutations. However, these female patients did not carry a *CDKL5* mutation. Some researchers have found no *CDKL5* mutations in patients with RTT (Huppke et al., 2005; Li et al., 2007). Previously, *CDKL5* mutations were analyzed in patients with both classic and atypical variants of RTT. However, mutations were identified only in patients with seizure onset before 6 months of age (Evans et al., 2005; Scala et al., 2005; Artuso et al., 2010). In another study, all patients with *CDKL5* mutations showed early onset seizures that began before 6 months of age (Erez et al., 2009). These findings suggest that development of early onset seizures is an essential clinical feature in patients with *CDKL5* mutations. The onset of epileptic seizures in the first 6 months distinguishes patients with *CDKL5* mutations from patients with typical RTT caused by *MECP2* mutations (Castren et al., 2011).

All previously reported *CDKL5* mutations were sporadic and were identified as de novo. Only a small numbers of mutations were recurrent (Castren et al., 2011). In this study, we observed eight *CDKL5* mutations that included six novel and two recurrent mutations. The phenotypic features of the patients with recurrent mutations are similar to those described previously (Sartori et al., 2009; Artuso et al., 2010).

Consistent with the findings of previous studies, we observed polymorphous seizures (i.e., myoclonic seizures, tonic seizures, and spasms) in our study. The clinical course of seizure development was also identical to the proposed three stages reported by Bahi-Buisson et al. (2008a) [i.e., stage I, early onset epilepsy (onset 1–10 weeks); stage II, epileptic encephalopathy with infantile spasms and hypsarrhythmia; stage III, seizure-free in estimated 50% of patients at late infantile period] because our Patient 7 showed good seizure control after 3 years of age. Artuso et al. (2010) reported that patients with *CDKL5* mutations showed no abnormalities on brain magnetic resonance imaging (MRI). However, our findings indicated mild frontal lobe atrophy in almost all patients. Therefore, this may be an additional clinical characteristic of patients with *CDKL5* mutations.

ACKNOWLEDGMENTS

DISCLOSURE

None of the authors has any conflict of interest to disclose. We confirm that we have read the Journal's position on issues involved in ethical publication and affirm that this report is consistent with those guidelines.

REFERENCES

Archer HL, Evans J, Edwards S, Colley J, Newbury-Ecob R, O'Callaghan F, Huyton M, O'Regan M, Tolmie J, Sampson J, Clarke A, Osborne J. (2006) CDKL5 mutations cause infantile spasms, early onset seizures, and severe mental retardation in female patients. *J Med Genet* 43:729–734.

Artuso R, Mencarelli MA, Polli R, Sartori S, Ariani F, Pollazzon M, Marozza A, Cilio MR, Specchio N, Vigevano F, Vecchi M, Boniver C, Bernardina BD, Parmeggiani A, Buoni S, Hayek G, Mari F, Renieri A, Murgia A. (2010) Early-onset seizure variant of Rett syndrome: definition of the clinical diagnostic criteria. *Brain Dev* 32:17–24.

Bahi-Buisson N, Kaminska A, Boddaert N, Rio M, Afenjar A, Gerard M, Giuliano F, Motte J, Heron D, Morel MA, Plouin P, Richelme C, des Portes V, Dulac O, Philippe C, Chiron C, Nabbout R, Bienvenu T. (2008a) The three stages of epilepsy in patients with CDKL5 mutations. *Epilepsia* 49:1027–1037.

Bahi-Buisson N, Nectoux J, Rosas-Vargas H, Milh M, Boddaert N, Girard B, Cances C, Ville D, Afenjar A, Rio M, Heron D, N'Guyen Morel MA, Arzimanoglou A, Philippe C, Jonveaux P, Chelly J, Bienvenu T. (2008b) Key clinical features to identify girls with CDKL5 mutations. *Brain* 131:2647–2661.

Bahi-Buisson N, Girard B, Gautier A, Nectoux J, Fichou Y, Saillour Y, Poirier K, Chelly J, Bienvenu T. (2010) Epileptic encephalopathy in a girl with an interstitial deletion of Xp22 comprising promoter and exon 1 of the CDKL5 gene. *Am J Med Genet B Neuropsychiatr Genet* 153B:202–207.

Castren M, Gaily E, Tengstrom C, Lahdetie J, Archer H, Ala-Mello S. (2011) Epilepsy caused by CDKL5 mutations. *Eur J Paediatr Neurol* 15:65–69.

Elia M, Falco M, Ferri R, Spalletta A, Bottitta M, Calabrese G, Carotenuto M, Musumeci SA, Lo Giudice M, Fichera M. (2008) CDKL5 mutations in boys with severe encephalopathy and early-onset intractable epilepsy. *Neurology* 71:997–999.

Erez A, Patel AJ, Wang X, Xia Z, Bhatt SS, Craigen W, Cheung SW, Lewis RA, Fang P, Davenport SL, Stankiewicz P, Lalani SR. (2009) Alu-specific microhomology-mediated deletions in CDKL5 in females with early-onset seizure disorder. *Neurogenetics* 10:363–369.

Evans JC, Archer HL, Colley JP, Ravn K, Nielsen JB, Kerr A, Williams E, Christodoulou J, Gecz J, Jardine PE, Wright MJ, Pilz DT, Lazarou L, Cooper DN, Sampson JR, Butler R, Whatley SD, Clarke AJ. (2005) Early onset seizures and Rett-like features associated with mutations in CDKL5. *Eur J Hum Genet* 13:1113–1120.

Fichou Y, Bieth E, Bahi-Buisson N, Nectoux J, Girard B, Chelly J, Chaix Y, Bienvenu T. (2009) Re: CDKL5 mutations in boys with severe encephalopathy and early-onset intractable epilepsy. *Neurology* 73:77–78; author reply 78.

Fichou Y, Nectoux J, Bahi-Buisson N, Chelly J, Bienvenu T. (2010) An isoform of the severe encephalopathy-related CDKL5 gene, including a novel exon with extremely high sequence conservation, is specifically expressed in brain. *J Hum Genet* 56:52–57.

Gomot M, Gendrot C, Verloes A, Raynaud M, David A, Yntema HG, Dessay S, Kalscheuer V, Frints S, Couvert P, Briault S, Blesson S, Toutain A, Chelly J, Desportes V, Moraine C. (2003) MECP2 gene mutations in non-syndromic X-linked mental retardation: phenotype-genotype correlation. *Am J Med Genet A* 123A:129–139.

Huppke P, Ohlenbusch A, Brendel C, Laccone F, Gartner J. (2005) Mutation analysis of the HDAC 1, 2, 8 and CDKL5 genes in Rett syndrome patients without mutations in MECP2. *Am J Med Genet A* 137:136–138.

Kalscheuer VM, Tao J, Donnelly A, Hollway G, Schwinger E, Kubart S, Menzel C, Hoeltzenbein M, Tommerup N, Eyre H, Harbord M, Haan E, Sutherland GR, Ropers HH, Gecz J. (2003) Disruption of the serine/threonine kinase 9 gene causes severe X-linked infantile spasms and mental retardation. *Am J Hum Genet* 72:1401–1411.

Li MR, Pan H, Bao XH, Zhang YZ, Wu XR. (2007) MECP2 and CDKL5 gene mutation analysis in Chinese patients with Rett syndrome. *J Hum Genet* 52:38–47.

Mari F, Azimonti S, Bertani I, Bolognese F, Colombo E, Caselli R, Scala E, Longo I, Grosso S, Pescucci C, Ariani F, Hayek G, Balestri P, Bergo A, Badaracco G, Zappella M, Broccoli V, Renieri A, Kilstrup-Nielsen C, Landsberger N. (2005) CDKL5 belongs to the same molecular pathway of MeCP2 and it is responsible for the early-onset seizure variant of Rett syndrome. *Hum Mol Genet* 14:1935–1946.

Mei D, Marini C, Novara F, Bernardina BD, Granata T, Fontana E, Parrini E, Ferrari AR, Murgia A, Zuffardi O, Guerrini R. (2010) Xp22.3 genomic deletions involving the CDKL5 gene in girls with early onset epileptic encephalopathy. *Epilepsia* 51:647–654.

Nabbout R, Dulac O. (2003) Epileptic encephalopathies: a brief overview. *J Clin Neurophysiol* 20:393–397.

Nabbout R, Dulac O. (2008) Epileptic syndromes in infancy and childhood. *Curr Opin Neurol* 21:161–166.

Nemos C, Lambert L, Giuliano F, Doray B, Roubertie A, Goldenberg A, Delobel B, Layet V, N'Guyen MA, Saunier A, Verneau F, Jonveaux P, Philippe C. (2009) Mutational spectrum of CDKL5 in early-onset encephalopathies: a study of a large collection of French patients and review of the literature. *Clin Genet* 76:357–371.

Pintaudi M, Baglietto MG, Gaggero R, Parodi E, Pessagno A, Marchi M, Russo S, Veneselli E. (2008) Clinical and electroencephalographic features in patients with CDKL5 mutations: two new Italian cases and review of the literature. *Epilepsy Behav* 12:326–331.

Sartori S, Di Rosa G, Polli R, Bettella E, Tricomi G, Tortorella G, Murgia A. (2009) A novel CDKL5 mutation in a 47,XXY boy with the early-onset seizure variant of Rett syndrome. *Am J Med Genet A* 149A:232–236.

Scala E, Ariani F, Mari F, Caselli R, Pescucci C, Longo I, Meloni I, Giachino D, Bruttini M, Hayek G, Zappella M, Renieri A. (2005) CDKL5/STK9 is mutated in Rett syndrome variant with infantile spasms. *J Med Genet* 42:103–107.

Shimojima K, Sugiura C, Takahashi H, Ikegami M, Takahashi Y, Ohno K, Matsuo M, Saito K, Yamamoto T. (2010) Genomic copy number variations at 17p13.3 and epileptogenesis. *Epilepsy Res* 89:303–309.

Van Esch H, Jansen A, Bauters M, Froyen G, Fryns JP. (2007) Encephalopathy and bilateral cataract in a boy with an interstitial deletion of Xp22 comprising the CDKL5 and NHS genes. *Am J Med Genet A* 143:364–369.

Zupanc ML. (2009) Clinical evaluation and diagnosis of severe epilepsy syndromes of early childhood. *J Child Neurol* 24:6S–14S.

SUPPORTING INFORMATION

Additional Supporting Information may be found in the online version of this article:

Table S1. The physical positions of BAC clones.

Table S2. Primer sequences for *CDKL5*.

Table S3. The results of aCGH.

Please note: Wiley-Blackwell is not responsible for the content or functionality of any supporting information supplied by the authors. Any queries (other than missing material) should be directed to the corresponding author for the article.

Craniofacial and Oral Features of Sotos Syndrome: Differences in Patients With Submicroscopic Deletion and Mutation of NSD1 Gene

Norimitsu Hirai,[1]* Kensuke Matsune,[2] and Hirofumi Ohashi[3]

[1]Department of Pediatric Dentistry, Nihon University Graduate School of Dentistry at Matsudo, Chiba, Japan

[2]Department of Pediatric Dentistry, Nihon University School of Dentistry at Matsudo, Chiba, Japan

[3]Division of Medical Genetics, Saitama Children's Medical Center, Saitama, Japan

Sotos syndrome is a well-known overgrowth syndrome caused by haploinsufficiency of NSD1 gene located at 5q35. There are two types of mutations that cause NSD1 haploinsufficiency: mutations within the NSD1 gene (mutation type) and a 5q35 submicroscopic deletion encompassing the entire NSD1 gene (deletion type). We investigated detailed craniofacial, dental, and oral findings in five patients with deletion type, and three patients with mutation type Sotos syndrome. All eight patients had a high palate, excessive tooth wear, crowding, and all but one patient had hypodontia and deep bite. Hypodontia was exclusively observed in the second premolars, and there were no differences between the deletion and mutation types in the number of missing teeth. Another feature frequently seen in common with both types was maxillary recession. Findings seen more frequently and more pronounced in deletion-type than in mutation-type included mandibular recession, scissors or posterior cross bite, and small dental arch with labioclination of the maxillary central incisors. It is noteworthy that although either scissors bite or cross bite was present in all of the deletion-type patients, neither of these was observed in mutation-type patients. Other features seen in a few patients include enamel hypoplasia (two deletion patients), and ectopic tooth eruption (one deletion and one mutation patients). Our study suggests that Sotos syndrome patients should be observed closely for possible dental and oral complications especially for malocculusion in the deletion-type patients. © 2011 Wiley Periodicals, Inc.

Key words: Sotos syndrome; NSD1; submicroscopic deletion; small dental arch; malocclusion; mandibular recession

How to Cite this Article:
Hirai N, Matsune K, Ohashi H. 2011. Craniofacial and oral features of Sotos syndrome: differences in patients with submicroscopic deletion and mutation of NSD1 gene.

Am J Med Genet Part A 155:2933–2939.

INTRODUCTION

Sotos syndrome is a congenital genetic disorder characterized by overgrowth starting before birth, specific facial manifestations (macrocephaly, prominent forehead, hypertelorism, downslanting palpebral fissures, and pointed chin), advanced bone age, and developmental impairment. Since its initial description by Sotos et al. [1964] several hundred patients have been reported to date.

It may be accompanied by a variety of complications, including cardiovascular, urinogenital, and ophthalmic malformations, skeletal abnormalities, and seizures. Dental and oral findings have been reported to include premature tooth eruption, hypodontia, enamel hypoplasia, excessive tooth wear, maxillary and mandibular recession, talon cusps, fused teeth, and expanded pulp cavity of deciduous teeth [Welbury and Fletcher, 1988; Cole and Hughes, 1994; Inokuchi et al., 2001; Gomes-Silva et al., 2006; Takei et al., 2007; Nishimura et al., 2008].

Kurotaki et al. [2002] reported that this syndrome is caused by haploinsufficiency of the NSD1 nuclear receptor SET domain containing protein 1 gene located on 5q35. There are two main types that cause NSD1 haploinsufficiency: mutations within the NSD1 gene, and a submicroscopic deletion in the region that contains the NSD1 gene (constant deletion of approximately 2.2 Mb including NSD1 and around 20 neighboring genes) [Kurotaki et al., 2002]. Nagai et al. [2003] investigated differences in clinical manifestations between these two types, and reported

2933

that major anomalies such as central nervous, cardiovascular, and urinogenital abnormalities are more common in the deletion-type. Their only reference to dental findings, however, stated that early tooth eruption occurred in both types with no significant difference.

The first detailed investigation of dental and oral findings seen in Sotos syndrome based on *NSD1* genetic diagnosis was carried out by Kotilainen et al. [2009]. They analyzed dental and oral findings from 13 patients with Sotos syndrome (all except one with the mutation type), including panoramic imaging, and reported the characteristic oral complications of Sotos syndrome, including hypodontia of the second premolars. We here report on the results of our investigation of detailed craniofacial, dental, and oral findings in five patients with deletion-type, and three patients with mutation-type Sotos syndrome.

MATERIALS AND METHODS
Patients

The eight patients comprised a group who underwent examination at Saitama Children's Medical Center. Five patients (three males, two females; age, 6–13 years) were identified as having a submicroscopic deletion on 5q35 including the *NSD1* gene, and three (all females; age, 6–10 years) were identified as having a mutation of the *NSD1* gene. Deletions were identified by fluorescence in situ hybridization (FISH) analysis of metaphase chromosomes from

peripheral blood, using a total of seven bacterial artificial chromosome (BAC) clones comprising the BAC clone that includes the *NSD1* gene (RP11-99N22) together with those toward the centromere (RP11-880A16, RP11-690I8, RP11-991B23) and toward the telomere (RP11-147K7, RP11-452O4, and RP11-158F10). The results showed that the same ~2 Mb deletion was present in all five patients. Mutation analysis using genomic DNA extracted from peripheral blood was performed by polymerase chain reaction (PCR) and direct sequencing of all translated regions for exon 2–23. The results identified mutations generating premature termination in both Patients 6 and 7, comprising a five base deletion (2053–2057delAAGTA) and a base deletion (5431delC), respectively, and a missense mutation (4991G>C) in Patient 8. Details of clinical manifestations are shown in Table I. This study protocol was approved by the Ethics Committee of Saitama Children's Medical Center and proper informed consents were obtained from the legal guardians of the patients.

Oral and Dental Studies

Physical examination and dental cast studies were used to evaluate palatal morphology, tooth calcification, dental arches, occlusion, tooth size, and tooth eruption status. Panoramic and lateral cephalometric radiographs reconstructed from multi-detector row computed tomography (MDCT) were also used to evaluate the relationship of craniofacial, dental and skeletal structures, and hypodontia [Hirai et al., 2010; Yamauchi et al., 2010]. Crown and

TABLE I. Clinical Manifestations of Eight Patients With Sotos Syndrome

	Deletion type patients					Mutation type patients		
	1	2	3	4	5	6	7	8
Gender	M	F	F	M	M	F	F	F
Ages (years)	7	8	6	7	13	7	10	6
Overgrowth	−	−	−	−	−	+	+	+
Intellectual disability	Moderate	Moderate	Moderate	Moderate	Moderate	Mild	−	Mild
Seizure	−	+	−	+	−	−	+	−
Craniofacial features								
Macrocephaly	+	+	+	−	+	+	+	−
Prominent forehead	+	+	+	+	+	+	+	−
Hypertelorism	+	+	+	+	+	+	+	+
Downslanting palpebral fissures	+	+	+	+	+	+	+	+
Pointed chin	+	+	+	+	+	+	+	+
Strabismus	+	+	+	−	−	+	−	−
Skeletal anomaly								
Scoliosis	−	−	−	+	+	−	+	+
Pes planovalgus	+	+	+	+	+	+	−	+
Cardiovascular anomaly	AR	PDA	−	PDA, ASD, VSD	−	VSD, CoA	MR	−
Urogenital anomaly	Hydronephrosis, VUR	−	−	−	−	Urethrocele	Hydronephrosis, hydroureter	−
Others	Hearing loss	Myelomeningocele, umblical hernia	−	−	−	−	−	−

M, male; F, female; AR, aortic regurgitation; PDA, patent ductus arteriosus; ASD, atrial septal defect; VSD, ventricular septal defect; CoA, coarctation of aorta; MR, mitral regurgitation; VUR, vesicoureteral reflux; +, present; −, absent.
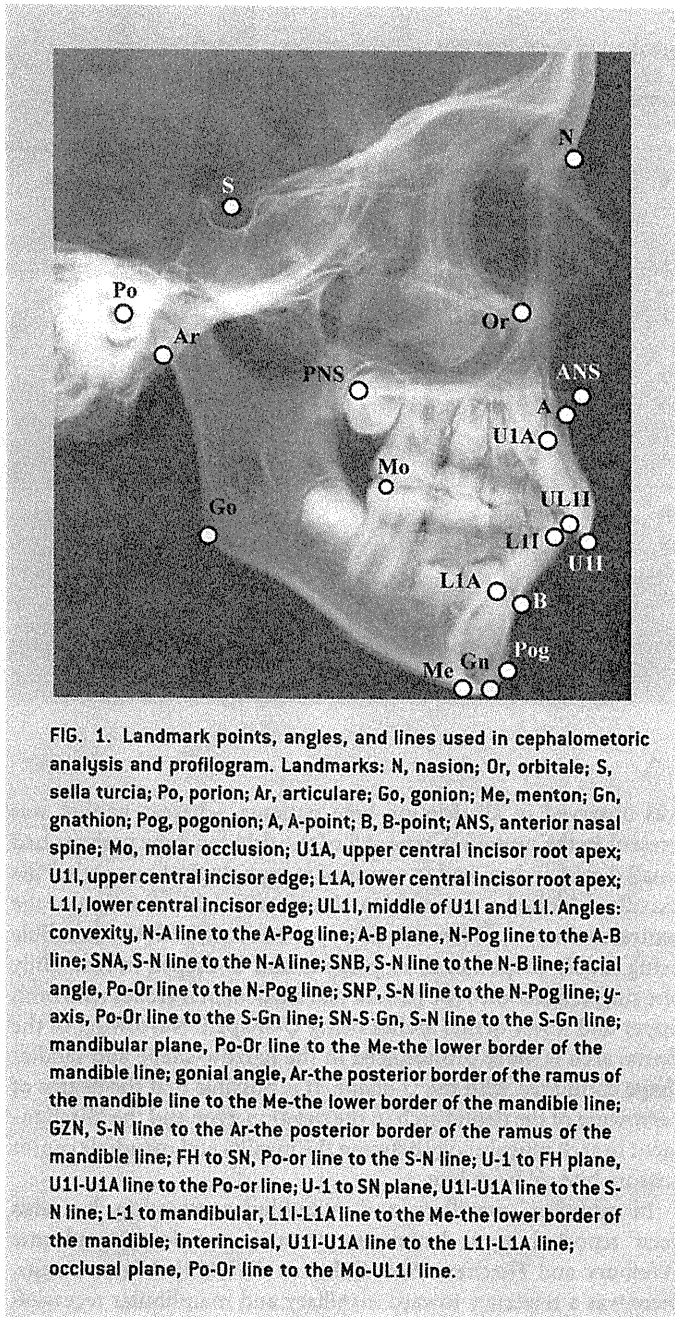
FIG. 1. Landmark points, angles, and lines used in cephalometoric analysis and profilogram. Landmarks: N, nasion; Or, orbitale; S, sella turcia; Po, porion; Ar, articulare; Go, gonion; Me, menton; Gn, gnathion; Pog, pogonion; A, A-point; B, B-point; ANS, anterior nasal spine; Mo, molar occlusion; U1A, upper central incisor root apex; U1I, upper central incisor edge; L1A, lower central incisor root apex; L1I, lower central incisor edge; UL1I, middle of U1I and L1I. Angles: convexity, N-A line to the A-Pog line; A-B plane, N-Pog line to the A-B line; SNA, S-N line to the N-A line; SNB, S-N line to the N-B line; facial angle, Po-Or line to the N-Pog line; SNP, S-N line to the N-Pog line; y-axis, Po-Or line to the S-Gn line; SN-S-Gn, S-N line to the S-Gn line; mandibular plane, Po-Or line to the Me-the lower border of the mandible line; gonial angle, Ar-the posterior border of the ramus of the mandible line to the Me-the lower border of the mandible line; GZN, S-N line to the Ar-the posterior border of the ramus of the mandible line; FH to SN, Po-or line to the S-N line; U-1 to FH plane, U1I-U1A line to the Po-or line; U-1 to SN plane, U1I-U1A line to the S-N line; L-1 to mandibular, L1I-L1A line to the Me-the lower border of the mandible; interincisal, U1I-U1A line to the L1I-L1A line; occlusal plane, Po-Or line to the Mo-UL1I line.

dental arch sizes were measured using a caliper with a resolution accuracy of 0.01 mm. Lateral cephalometric analysis was performed based on the method developed by Iizuka and Ishikawa [1957] (Fig. 1). All data in this study (tooth size, dental arch form size, and cephalometric findings) were compared with standard values for Japanese individuals [Otsubo, 1957; Otsubo et al., 1964].

RESULTS

Oral and dental anomalies noted in eight patients are summarized in Table II. All eight patients had a high palate, crowding, and excessive tooth wear. All but one (Patient 1 with NSD1 deletion) had

hypodontia exclusively in the second premolars. There were no differences between the deletion-type and mutation-types in the number of missing teeth (mean number of missing teeth was 2 in the deletion-type and 2.6 in the mutation-type) (Fig. 2). The results of cephalometric analysis showed that among the five deletion-type patients, maxillary and mandibular recession was present in three and maxillary recession alone in one, whereas among the three mutation-type patients maxillary and mandibular recession was present in one and maxillary recession alone in one. The deletion-type was regarded as having a stronger tendency for mandibular recession (Table III). In terms of occlusion, crowding was present in all patients, and deep bite was seen in all but one (Patient 2 with NSD1 deletion). It is noteworthy that although either scissors bite (Patients 1, 3, and 4) or cross bite (Patients 2 and 5) was present in all of the deletion-type patients, neither of these was observed in mutation-type patients (Fig. 3).

Small dental arch was present in all the deletion-type patients and one mutation-type patient (Table IV). In terms of morphological categories of small dental arch, the maxilla exhibited a narrow dental arch with labioclination of the central incisors in all five deletion-type patients, with the mandible being saddle-shaped in three patients and U-shaped in two, while the mutation-type patient had U-shaped upper and lower dental arches (Fig. 4). In terms of tooth size, both microdontia and macrodontia were occasionally seen in both the deletion-type and mutation-types, but no characteristic findings were present in either type (data not shown). Enamel hypoplasia was present in two out of the five deletion-type patients (Patients 2 and 3), but was not present in the mutation-type. In addition, ectopic eruption of the first molar was present in one deletion-type patient (Patient 4, right mandibular) and one mutation-type patient (Patient 6, bilateral maxillary). Some representative photographs of oral and dental anomalies noted in patients studied are shown in Figure 5.

DISCUSSION

The oral manifestations observed in common with both deletion and mutation type Sotos syndrome patients noted here were a high palate, excessive tooth wear, recession of maxilla, deep bite, crowding, and hypodontia. Hypodontia has been previously described by several authors [Inokuchi et al., 2001; Callnan et al., 2006; Gomes-Silva et al., 2006; Nishimura et al., 2008]. Kotilainen et al. [2009] recently investigated 13 patients with Sotos syndrome (12 patients with NSD1 mutations and one with NSD1 deletion) and found one or more premolar teeth were absent in 9 out of 13 patients (8 out of 12 mutation patients and one deletion-type patient). Based on the observation that the deletion patient had the most severe phenotype of tooth agenesis, involving not only the second premolars and the third molars, but also one mandibular incisor, they noted the possibility that patient with the NSD1 deletion had the most severe tooth agenesis. In our study, however, which included five deletion-type patients, although similar high rates of hypodontia were observed in both the deletion-type and mutation-type, we did not observe any difference in severity in either the deletion-type or mutation-type.

One noteworthy difference between the deletion-type and mutation-type was the fact that either scissors bite or cross bite

TABLE II. Oral and Dental Anomalies in Eight Patients

Oral anomalies	Deletion type patients					Mutation type patients			Total	
	1	2	3	4	5	6	7	8	Deletion type	Mutation type
High palate	+	+	+	+	+	+	+	+	5/5	3/3
Excessive tooth wear	+	+	+	+	+	+	+	+	5/5	3/3
Hypodontia	−	+	+	+	+	+	+	+	4/5	3/3
Maxillary recession	+	−	+	+	+	+	+	−	4/5	2/3
Mandibular recession	−	−	+	+	+	−	+	−	3/5	1/3
Malocclusion										
Scissors bite	+	−	+	+	−	−	−	−	3/5	0/3
Cross bite	−	+	−	−	+	−	−	−	2/5	0/3
Deep bite	+	−	+	+	+	+	+	+	4/5	3/3
Crowding	+	+	+	+	+	+	+	+	5/5	3/3
Small dental arch	+	+	+	+	+	−	+	−	5/5	1/3
Maxilla	N	N	N	N	N	U	U	U		
Mandibula	S	U	S	S	U	U	U	U		
Labioclination of maxillary central incisor	+	+	+	+	+	−	−	−	5/5	0/3
Enamel hypoplasia	−	+	+	−	−	−	−	−	2/5	0/3
Ectopic tooth eruption	−	−	−	+	−	+	−	−	1/5	1/3

N, narrow dental arch; U, U-shaped dental arch; S, saddle-shaped dental arch; +, present; −, absent.

Deletion type

Patient 1

Patient 2

Patient 3

Patient 4

Patient 5

Mutation type

Patient 6

Patient 7

Patient 8

	Right								Left						
Upper	7	6	5	4	3	2	1	1	2	3	4	5	6	7
Lower	7	6	5	4	3	2	1	1	2	3	4	5	6	7

FIG. 2. Hypodontia in eight patients with Sotos syndrome. ●, Congenitally missing teeth.

was observed in all deletion-type patients, whereas neither was present in the mutation-type. All of the deletion-type patients had small dental arches, and in terms of morphological categories, the maxilla exhibited a narrow dental arch with labioclination of the central incisors in all five deletion-type patients, with the mandible being saddle-shaped in three patients and U-shaped in two. Only one single mutation-type patient had small dental arches with both upper and lower dental arches being U-shaped. Narrowing of the dental arch is more pronounced in the narrow-shape and saddle-shape compared with the U-shape. It is possible that the degree of narrowing of the dental arch in the deletion-type and the misalignment in arch morphology between the maxilla and mandible causes scissors bite or cross bite.

In addition, maxillary and mandibular recession has also been reported as a dental manifestation of Sotos syndrome [Welbury and Fletcher, 1988; Takei et al., 2007]. In our results, there was a tendency toward maxillary and mandibular recession in the deletion-type and maxillary recession in the mutation-type. Based on these findings, there was a tendency for maxillary recession to occur in both the deletion-type and mutation-type, but there was also a tendency toward the occurrence of mandibular recession in the deletion-type. Taken in conjunction with the pronounced mandibular recession seen in the deletion-type on cephalometric analysis, mandibular malformations, including those of the dental arch, may be regarded as characteristic of the deletion-type. The cause is unknown, but in the deletion-type, minute genome imbalances, involving considerable number of genes other than the NSD1 gene, may either: (1) directly cause deficient growth of the mandibular area; or (2) secondarily cause malocclusion or abnormal dental arch morphology as a result of dysfunction of the perioral muscles associated with more

TABLE III. Lateral Cephalometric Analysis With MDCT of Eight Patients

	Deletion type patients					Mutation type patients		
	1	2	3	4	5	6	7	8
Skeletal								
Covexity	−2.56	−1.05	−0.66	−1.80	−1.95	−4.56	−2.52	−2.94
A−B plane	−1.12	−3.96	1.68	−0.32	1.40	2.15	1.96	2.56
SNA	−2.54	1.24	−2.28	−3.45	−2.32	−2.69	−3.18	−1.63
SNB	−1.80	1.71	−3.31	−3.18	−2.84	−0.76	−2.29	−0.07
Facial angle	0.68	−3.23	−0.47	0.38	0.34	0.38	−1.55	1.43
SNP	−0.71	1.77	−1.76	−1.16	−0.63	0.02	−2.22	0.11
Y-axis	−0.50	−0.37	−0.38	−0.08	0.17	−0.36	1.29	−1.34
SN-S-Gn	3.08	−1.30	0.32	3.86	0.93	0.22	1.86	−0.30
Mandibular plane	1.29	1.05	−1.47	0.30	1.12	−0.58	1.98	−0.29
Gonial angle	6.24	−0.15	−4.06	−5.27	0.73	0.29	0.44	3.06
GZN	0.77	0.09	3.01	2.84	1.19	−0.37	1.52	−0.27
FH to SN	2.38	−1.15	0.71	2.55	0.98	0.52	0.97	1.37
Denture								
U-1 to FH plane	1.30	1.37	2.94	0.30	0.72	−0.47	0.50	0.69
U-1 to SN plane	0.51	1.87	2.56	−0.52	0.24	−0.64	−0.46	0.21
L-1 to mandibular	−2.24	−0.47	0.98	−1.47	−1.64	−2.39	−0.46	−1.93
Interincisal	−0.07	−1.07	−1.53	0.46	0.22	1.90	−0.83	0.71
Occlusal plane	−0.99	1.09	−0.76	−0.24	2.97	−1.37	1.35	−0.49

Unit, SD.
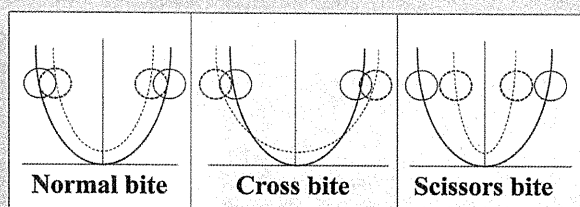

Normal bite   **Cross bite**   **Scissors bite**

FIG. 3. Schematic representations of normal and abnormal occlusions.————, Maxillary dental arch; ------, mandibular dental arch; ◯, maxillary first molar; ◌, mandibular first molar.

pronounced developmental impairment [Grabowski et al., 2007a,b; Stahl et al., 2007].

Enamel hypoplasia has also been reported as a dental manifestation of Sotos syndrome [Inokuchi et al., 2001]. Kotilainen et al. [2009] reported enamel hypoplasia in four out of 13 patients (all mutation type). In our study, enamel hypoplasia was present in two out of five deletion-type patients, but not in any mutation-type patients. Enamel hypoplasia is thought to be a common manifestation that can occasionally occur in both the deletion-type and mutation-type rather than a manifestation that is prone to occur in either type.

As mild to moderate intellectual disability is common in Sotos syndrome, conventional panoramic, and cephalometric studies

TABLE IV. Dental Arch Measurements in Eight Patients

	Deletion type patients					Mutation type patients		
	1	2	3	4	5	6	7	8
Maxillary								
Wc	−0.55	Deciduous	0.04	Deciduous	1.79	−1.75	0.61	−1.30
W6	−3.76	−3.59	0.02	−4.18	−3.11	−1.73	−2.04	−1.76
L16	2.68	1.33	2.88	1.02	−0.69	1.44	0.14	−1.36
Mandibular								
Wc	Deciduous	Deciduous	−1.00	Deciduous	−0.73	−1.81	−2.70	−0.30
W6	−4.82	−2.51	−2.16	−4.45	−3.38	−1.57	−4.34	0.96
L16	0.81	1.32	1.85	0.63	−3.40	0.20	−2.07	0.56

Unit, SD.
The W_c and W_6 represent the distance between the primary cuspids (the cuspids), and the first molars, respectively. The L_{16} represents the length from the mesial surface of the first molars to central point of incisors.
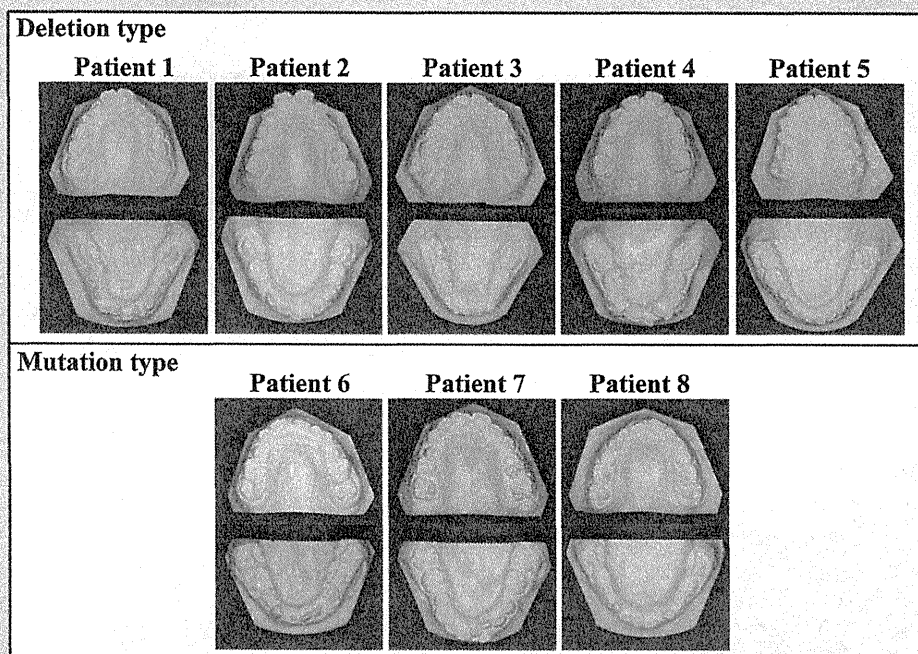
FIG. 4. Dental arch shapes of eight patients. Upper panel: maxillary dental casts, lower panel: mandibular dental casts. A narrow maxillary dental arch with labioclination of the central incisors is noted in all five deletion type patients, with the mandibula being saddle-shaped in three patients (Patients 1, 3, and 4) and U-shaped in two (Patients 2 and 5), while U-shaped upper and lower dental arches are noted in all three mutation-type patients (Patients 6, 7, and 8).
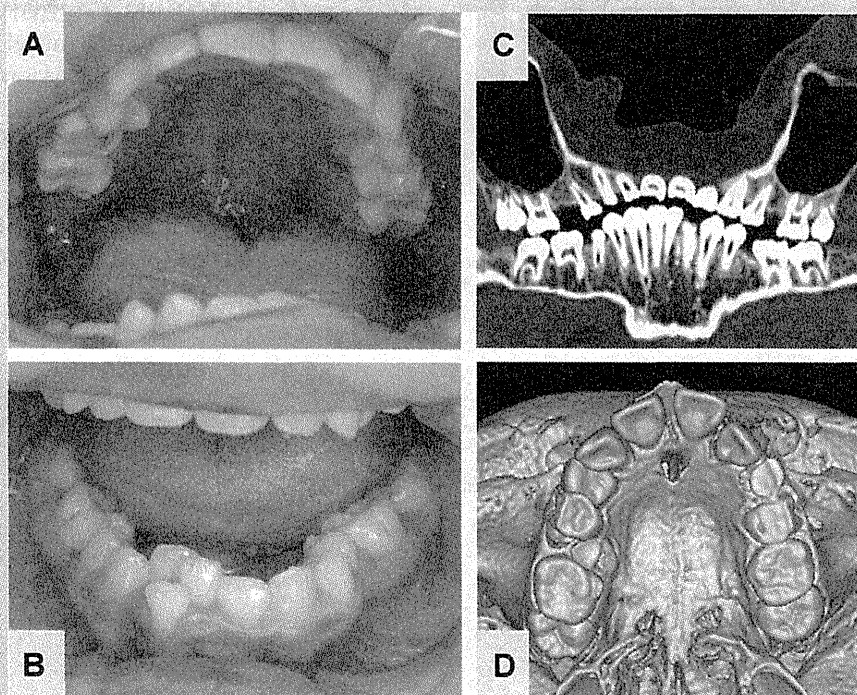

FIG. 5. Oral photographs (A,B) and MDCT-synthesized panoramic radiograph (C) of Patient 7 at age of 10 years and MDCT-synthesized upper dental arch of Patient 6 at age of 7 years (D). Note: high palate, malocclusion, small dental arch, excessive tooth wear (A,B), missing upper second premolars on both side and lower left second premolar (C), ectopic tooth eruption of first molars on both side (D).

were often difficult to perform in childhood. Thus, in this study, MDCT was used as a substitute for cephalometric radiographs and panoramic radiographs, and by which maxillofacial manifestations could be accurately evaluated [Hirai et al., 2010; Yamauchi et al., 2010].

In view of oral and dental management, we would like to provide recommendations as follows: periodic dental check up to prevent dental caries or gingivitis should be started early after one or more deciduous teeth have erupted. Around age 7 years, detailed oral and dental evaluations, including dental cast studies and MDCT, is recommended for possible hypodontia and malocclusion. If the patient has hypodontia, preceding deciduous tooth (teeth) should be maintained as long as possible with proper care. Although malocclusion like scissors bite and cross bite requires early treatment, including expansion of upper or lower jaw, to prevent craniofacial disabilities such as facial asymmetry and temporomandibular joint dysfunction, the treatment should be carefully decided based on consideration of capability of cooperation of the patients.

In conclusion, features seen more frequently and more pronounced form in deletion-type than in mutation-type were small dental arch with labioclination of the maxillary central incisors, mandibular recession, and scissors or posterior cross bite. Sotos syndrome patients should be followed closely for possible dental and oral complications especially for malocculusion in the deletion-type.

ACKNOWLEDGMENTS

REFERENCES

Callnan AP, Anand P, Sheehy EC. 2006. Sotos syndrome with hypodontia. Inter J Paediatri Dent 16:143–146.

Cole TRP, Hughes HE. 1994. Sotos syndrome: A study of the diagnostic criteria and natural history. J Med Genet 31:20–32.

Gomes-Silva JM, Ruviere DB, Segatto RA, de Queiroz AM, de Freitas AC. 2006. Sotos syndrome: A case report. Spec Care Dentist 26:257–262.

Grabowski R, Kundt G, Stahl F. 2007a. Interrelation between occlusal findings and orofacial myofunctional status in primary and mixed dentition: Part III: Interrelation between malocclusions and orofacial dysfunctions. J Orofac Orthop 68:462–476.

Grabowski R, Stahl F, Gaebel M, Kundt G. 2007b. Relationship between occlusal findings and orofacial myofunctional status in primary and mixed dentition. Part I: Prevalence of malocclusions. J Orofac Orthop 68:26–37.

Hirai N, Yamauchi T, Matsune K, Kobayashi R, Yabe H, Ohashi H, Maeda T. 2010. A comparison between two dimensional and three dimensional cephalometry on lateral radiographs and multi detector row computed tomography scans of human skulls. Int J Oral-Med Sci 9:101–107.

Iizuka T, Ishikawa F. 1957. Normal standards for various cephalometric analysis in Japanese adults. Nippon Kyosei Shika Gakkai Zasshi 16:4–12.

Inokuchi M, Nomura J, Mtsumura Y, Sekida M, Tagawa T. 2001. Sotos syndrome with enamel hypoplasia: A case report. J Clin Pediatr Dent 25:313–316.

Kotilainen J, Pohjola P, Pirinen S, Arte S, Nieminen P. 2009. Premolar hypodontia is a common feature in Sotos syndrome with a mutation in the NSD1 gene. Am J Med Genet Part A 149A:2409–2414.

Kurotaki N, Imaizumi K, Harada N, Masuno M, Kondoh T, Nagai T, Ohashi H, Naritomi K, Tsukahara M, Makita Y, Sugimoto T, Sonoda T, Hasegawa T, Chinen Y, Tomita HH, Kinoshita A, Yoshiura KK, Ohta T, Kishino T, Fukushima Y, Niikawa N, Matsumoto N. 2002. Haploinsufficiency of NSD1 causes Sotos syndrome. Nat Genet 30:365–366.

Nagai T, Matsumoto N, Kurotaki N, Harada N, Niikawa N, Ogata T, Imaizumi K, Kurosawa K, Kondoh T, Ohashi H, Tsukahara M, Makita Y, Sugimoto T, Sonoda T, Yokoyama T, Uetake K, Sakazume S, Fukushima Y, Naritomi K. 2003. Sotos syndrome and haploinsufficiency of NSD1: Clinical features of intragenic mutations and sub microscopic deletions. J Med Genet 40:285–289.

Nishimura K, Mori Y, Yamauchi M, Kamakura N, Homma H, Namura H, Miyamoto E, Matsumoto M, Shintani S, Ooshima T. 2008. Sotos syndrome with oligodontia: A case report. Pediatric Dent J 18:187–191.

Otsubo J. 1957. A study on the tooth material in Japanese adults of normal occlusion, its relationship to coronal and basal arches. Nippon Kyosei Shika Gakkai Zasshi 16:36–46.

Otsubo J, Ishikawa F, Kuwahara Y. 1964. A longitudinal study of dental development between 6–13 years of age: Growth changes of dentition. Nippon Kyosei Shika Gakkai Zasshi 23:182–190.

Sotos JF, Dodge PR, Muirhead Dl, Crawford JD, Talbot NB. 1964. Cerebral gigantism in childhood. A syndrome of excessively rapid growth with acromegatic features and a nonprogressive neurologic disorder. N Engl J Med 271:109–116.

Stahl F, Grabowski R, Gaebel M, Kundt G. 2007. Relationship between occlusal findings and orofacial myofunctional status in primary and mixed dentition. Part II: Prevalence of orofacial dysfunctions. J Orofac Orthop 68:74–90.

Takei K, Sueishi K, Yamaguchi H, Ohtawa Y. 2007. Dentofacial growth in patients with Sotos syndrome. Bull Tokyo Dent Coll 48:73–85.

Welbury RR, Fletcher HJ. 1988. Cerebral gigantism (Sotos syndrome) two case reports. J Paediatr Dent 4:41–44.

Yamauchi T, Hirai N, Matsune K, Kobayashi R, Yabe H, Ohashi H, Maeda T. 2010. Accuracy of tooth development stage, tooth size and dental arch width in multi detector row computed tomography scans of human skulls. Int J Oral Med Sci 9:108–114.